

# A Demonstration of Dual Spacecraft Tracking Conducted With the Viking Spacecraft During the Approach Phase

C. C. Chao

Navigation Systems Section

*The potential improvements in navigation capability of dual spacecraft tracking have been demonstrated using Viking approach data. Under unfavorable conditions of large plasma noise, low spacecraft declination and large Earth-spacecraft distance, the dual spacecraft tracking technique improved the Viking B approach accuracy based on short-arc radio metric data, by a factor of 7, to less than 200 km at Mars Orbit Insertion (MOI) minus 3 days. From the results of an analytical expansion and the Viking demonstration with a large intentional error in Mars ephemeris, we are able to conclude that dual spacecraft data types are insensitive to ephemeris error. Results also reveal the potential reduction of tracking time requirements during planet approach.*

## I. Introduction

For interplanetary space missions involving two spacecraft, such as Viking or Voyager, significant navigation advantages may sometimes be achieved (at least for the trailing vehicle) by determining the orbit of one relative to the other, or otherwise combining the data from the two spacecraft, rather than treating them independently as has been done in the past. Analysis of the dual spacecraft navigation concept and results of a demonstration using data from the early cruise phase of the Viking mission were reported in Refs. 1 and 2. Results from the analysis in Ref. 2 show that:

- (1) Dual spacecraft data types, which are relatively insensitive to platform parameter errors, transmission media effects, low declination problems, and ephemeris errors, may improve navigational capabilities by a factor of 5 to 10, under the conditions of small angular separation ( $\leq 3$  deg) of the two spacecraft and well determined trajectory of the reference spacecraft.
- (2) Dual spacecraft tracking has the potential of significantly reducing DSN tracking time requirements.

This paper presents new analytical models for the dual spacecraft data types and reports new results from a more recent demonstration conducted during the approach phase of the Viking mission. The demonstration was based on data taken two weeks before MOI of the second Viking spacecraft, when the first spacecraft had been in orbit for several weeks and its orbit relative to Mars was well determined. The demonstration was designed to show that the approaching probe could be tied accurately to the planet through the orbiter.

## II. Analytic Expansion of Dual Spacecraft Data

The information content of dual spacecraft data has been analyzed in Refs. 1 and 2, and the reduction in sensitivity to platform parameter errors, low declination problems and transmission media effects are clearly understood. However, the cancellation of ephemeris error during a dual spacecraft flyby has not been investigated. Furthermore, the previous analysis using a Hamilton-Melbourne (Ref. 3) type of approximation

ignores higher order terms, some of which become important after differencing.

During the approach phase, the planetocentric distances of the two spacecraft are much smaller than the geocentric distances, as shown in Fig. 1. The range and range-rate observables ( $\rho$  and  $\dot{\rho}$ ) from one spacecraft may be expressed in terms of planetocentric coordinates  $\vec{r}$ , the geocentric position of the planet  $\vec{R}$ , and the position vector of the tracking station  $\vec{s}$  as follows:

$$\rho = [(\vec{R} + \vec{r} - \vec{s}) \cdot (\vec{R} + \vec{r} - \vec{s})]^{1/2}$$

$$\dot{\rho} = \frac{\vec{\rho} \cdot \dot{\vec{\rho}}}{\rho} = \frac{1}{\rho} (\vec{R} + \vec{r} - \vec{s}) \cdot (\dot{\vec{R}} + \dot{\vec{r}} - \dot{\vec{s}})$$

The above equation for the range observables may be rewritten as

$$\begin{aligned} \rho &= [R^2 + r^2 + s^2 + 2(\vec{R} \cdot \vec{r} - \vec{R} \cdot \vec{s} - \vec{r} \cdot \vec{s})]^{1/2} \\ &= R(1 + \epsilon)^{1/2} \end{aligned}$$

where

$$\epsilon = 2 \left( \frac{\vec{R} \cdot \vec{r} - \vec{R} \cdot \vec{s} - \vec{r} \cdot \vec{s}}{R^2} \right) + \left( \frac{r}{R} \right)^2 + \left( \frac{s}{R} \right)^2$$

When a spacecraft is encountering a planet,  $\epsilon$  is small because

$$1 \gg \frac{r}{R} \gg \frac{s}{R}$$

After expansion we have

$$\rho = R \left( 1 + \frac{1}{2} \epsilon - \frac{1}{8} \epsilon^2 + \dots \right)$$

Then to the first order in  $s/R$  and second order in  $r/R$  we have

$$\begin{aligned} \rho &= R + (x - s_x) \cos \delta' \cos \alpha' + (y - s_y) \cos \delta' \sin \alpha' \\ &\quad + (z - s_z) \sin \delta' + \frac{1}{2} r \left( \frac{r}{R} \right) \sin^2 \psi \\ &\quad - \left( s_x \frac{x}{R} + s_y \frac{y}{R} + s_z \frac{z}{R} \right) \end{aligned} \quad (1)$$

where  $\psi$  is the angle between vectors  $\vec{R}$  and  $\vec{r}$ .

Similarly the range rate observable may be expanded as

$$\begin{aligned} \dot{\rho} &= \frac{1}{R} \left( 1 - \frac{1}{2} \epsilon + \frac{3}{8} \epsilon^2 + \dots \right) (\vec{R} \cdot \dot{\vec{R}} + \vec{R} \cdot \dot{\vec{r}} - \vec{R} \cdot \dot{\vec{s}} \\ &\quad + \vec{r} \cdot \dot{\vec{R}} + \vec{r} \cdot \dot{\vec{r}} - \vec{r} \cdot \dot{\vec{s}} \\ &\quad - \vec{s} \cdot \dot{\vec{R}} - \vec{s} \cdot \dot{\vec{r}} + \vec{s} \cdot \dot{\vec{s}}) \end{aligned}$$

or

$$\begin{aligned} \dot{\rho} &= C + \left( \cos \delta' \cos \alpha' + \frac{x}{R} - \frac{s_x}{R} \right) \dot{x} \\ &\quad + \left( \cos \delta' \sin \alpha' + \frac{y}{R} - \frac{s_y}{R} \right) \dot{y} \\ &\quad + \left( \sin \delta' + \frac{z}{R} - \frac{s_z}{R} \right) \dot{z} + E_x \frac{x}{R} \\ &\quad + E_y \frac{y}{R} + E_z \frac{z}{R} \end{aligned} \quad (2)$$

where  $C$  and  $E_x, E_y, E_z$  are functions of planet and station location coordinates

$$C = (\dot{R}_x - \dot{s}_x) \left( \cos \delta' \cos \alpha' - \frac{s_x}{R} \right)$$

$$+ (\dot{R}_y - \dot{s}_y) \left( \cos \delta' \sin \alpha' - \frac{s_y}{R} \right)$$

$$+ \dot{R}_z \left( \sin \delta' - \frac{s_z}{R} \right)$$

$$E_x = (\dot{R}_x - \dot{s}_x) (1 - \cos^2 \delta' \cos^2 \alpha')$$

$$- \frac{1}{2} (\dot{R}_y - \dot{s}_y) \cos^2 \delta' \sin 2\alpha'$$

$$- \frac{1}{2} \dot{R}_z \sin 2\delta' \cos \alpha'$$

$$\begin{aligned}
E_y &= -\frac{1}{2} (\dot{R}_x - \dot{s}_x) \cos^2 \delta' \sin 2\alpha' \\
&\quad + (\dot{R}_y - \dot{s}_y) (1 - \cos^2 \delta' \sin^2 \alpha') \\
&\quad - \frac{1}{2} \dot{R}_z \sin 2\delta' \sin \alpha' \\
E_z &= -\frac{1}{2} (\dot{R}_x - \dot{s}_x) \sin 2\delta' \cos \alpha' \\
&\quad - \frac{1}{2} (\dot{R}_y - \dot{s}_y) \sin 2\delta' \sin \alpha' + \dot{R}_z \cos^2 \delta'
\end{aligned}$$

If the two spacecraft are being tracked simultaneously from the same site, a new data type may be formed by differencing the corresponding observables from the two spacecraft.

$$\begin{aligned}
\Delta\rho &= \rho - \rho_1 = \cos \delta' \cos \alpha' (x - x_1) + \cos \delta' \sin \alpha' (y - y_1) \\
&\quad + \sin \delta' (z - z_1) + \frac{1}{2} r \left( \frac{r}{R} \right) \sin^2 \psi - \frac{1}{2} r_1 \left( \frac{r_1}{R} \right) \sin^2 \psi_1 \\
&\quad + s_x \frac{(x - x_1)}{R} + s_y \frac{(y - y_1)}{R} + s_z \frac{(z - z_1)}{R} \quad (3)
\end{aligned}$$

$$\begin{aligned}
\Delta\dot{\rho} &= \dot{\rho} - \dot{\rho}_1 = \left( \cos \delta' \cos \alpha' - \frac{s_x}{R} \right) (\dot{x} - \dot{x}_1) \\
&\quad + \left( \cos \delta' \sin \alpha' - \frac{s_y}{R} \right) (\dot{y} - \dot{y}_1) \\
&\quad + \left( \sin \delta' - \frac{s_z}{R} \right) (\dot{z} - \dot{z}_1) + \frac{1}{R} (x\dot{x} + y\dot{y} + z\dot{z} - x_1\dot{x}_1 - y_1\dot{y}_1 \\
&\quad - z_1\dot{z}_1) + E_x \frac{(x - x_1)}{R} + E_y \frac{(y - y_1)}{R} \\
&\quad + E_z \frac{(z - z_1)}{R} \quad (4)
\end{aligned}$$

The above data types are called two spacecraft 2-station range and range rate (doppler). It is clear that the terms,  $R$  and  $C$  in Eqs. (1) and (2), which are sensitive to planet ephemeris and

station location errors, are removed. The ephemeris and station location coordinates in the above equations are multiplied by the small factors of  $(x - x_1)/R$  or  $1/R$  etc., thus these errors could be reduced accordingly. Furthermore, the quality of the above differenced data is improved due to the cancellation of transmission media effects. However, they are still sensitive to unmodeled spacecraft accelerations, i.e., attitude-control gas leaks and solar pressure anomalies. These noises may be removed by differencing the data simultaneously obtained from two widely separated stations. Consistent with Ref. 2, the single spacecraft 2-station data type and two spacecraft 4-station data types are to be derived next.

When simultaneous 2-station tracking from one spacecraft is assumed, the differenced range and range rate may be obtained from Eqs. (1) and (2) and expressed in terms of baseline coordinates  $r_B, \alpha_B$  and  $z_B$ .

$$\begin{aligned}
D\rho &= r_B \cos \delta' \sin (\alpha_B - \alpha') + z_B \sin \delta' \\
&\quad + r_B \left( \frac{x}{R} \sin \alpha_B + \frac{y}{R} \cos \alpha_B \right) + z_B \frac{z}{R} \quad (5)
\end{aligned}$$

$$\begin{aligned}
D\dot{\rho} &= \omega r_B \cos \delta' \cos (\alpha_B - \alpha') + \frac{\omega r_B}{R} [G_x x + G_y y + G_z z] \\
&\quad + \frac{r_B}{R} [\sin \alpha_B \dot{x} + \cos \alpha_B \dot{y}] + \frac{z_B}{R} \dot{z} \quad (6)
\end{aligned}$$

where

$$\begin{aligned}
G_x &= \sin \alpha_B (1 - \cos^2 \delta' \cos^2 \alpha') - \frac{1}{2} \cos \alpha_B \cos^2 \delta' \sin 2\alpha' \\
G_y &= -\frac{1}{2} \sin \alpha_B \cos^2 \delta' \sin 2\alpha' + \cos \alpha_B (1 - \cos^2 \alpha' \cos^2 \delta') \\
G_z &= -\frac{1}{2} \sin \alpha_B \sin 2\delta' \cos \alpha' - \frac{1}{2} \cos \alpha_B \sin 2\delta' \sin \alpha'
\end{aligned}$$

The above data types are the one spacecraft 2-station range and range rate.

The first two terms in Eq. (5) and the first term in Eq. (6) contain the angular position of the planet ( $\alpha', \delta'$ ) and therefore, the data are sensitive to planet ephemeris errors. In addition, the baseline parameters  $r_B, z_B$  and  $\alpha_B$  are another

major error source. After the second differencing, the 2 spacecraft 4-station range and rate are:

$$D\rho - D\rho_1 = r_B \left[ \sin \alpha_B \left( \frac{x - x_1}{R} \right) + \cos \alpha_B \left( \frac{y - y_1}{R} \right) \right] + z_B \frac{z - z_1}{R} \quad (7)$$

$$D\dot{\rho} - D\dot{\rho}_1 = r_B \left\{ \omega \left[ G_x \frac{(x - x_1)}{R} + G_y \frac{(y - y_1)}{R} + G_z \frac{(z - z_1)}{R} \right] + \sin \alpha_B \frac{(\dot{x} - \dot{x}_1)}{R} + \cos \alpha_B \frac{(\dot{y} - \dot{y}_1)}{R} \right\} + z_B \frac{(\dot{z} - \dot{z}_1)}{R} \quad (8)$$

With those common terms removed, the dual spacecraft 4-station data types are not only insensitive to planet ephemeris and station location errors, but also free from noises resulting from transmission media and unmodeled spacecraft accelerations. This clean data type thus can accurately tie one spacecraft to the other.

The above expansions provide some insight into various observables and are helpful in examining the information content of the dual spacecraft data types. Due to the fact that the planet relative state of the two encountering spacecraft change appreciably over a short time (one day), the information content from a single pass of data cannot be extracted in the same manner as in Ref. 2. However, the sensitivities to planet ephemeris error and station location uncertainties may be seen from the partial derivatives which may be easily derived from the above equations. These approximate equations of observables and partial derivatives may be useful for performing certain types of preliminary analysis of dual spacecraft tracking during a planet approach.

Although the potential reduction in sensitivities to planet ephemeris and station location errors has been shown through the analytical expansion, a simplified example based on those equations may be helpful. If  $\vec{r}$  and  $\vec{r}_1$  are assumed fixed, one may compute using Eqs. (1) to (8) the equivalent error in each observable which corresponds to (or would be induced by) a given ephemeris error. If the computed bias is large compared with the inherent accuracy of the observable, then the ephemeris error will corrupt the estimate of  $\vec{r}$ . A simplified

example of this type of analysis for the Saturn approach of the Voyager mission is shown by the upper charts of Fig. 2. The two Voyager spacecraft will be separated by 9 deg when the second probe approaches Saturn in 1981. Most of the 2000 km (conservative estimate) ephemeris error cancels as the dual spacecraft data types are differenced (Fig. 2). For the dual spacecraft 2-station data type, the bias left in the differenced data is still quite large (see upper left chart of Fig. 2). This is due to the fact that the cancellation of the ephemeris error in right ascension and declination is not as effective as that along the line-of-sight direction that may be seen from Eq. (4). Because of the asymmetry of the two sets of state parameters,  $x, y, \dots, x_1, y_1, \dots$ , in Eq. (4), this sensitivity may be removed by estimating both spacecraft. After regression analysis one may lead to the following relations:

$$\frac{\partial x}{\partial \delta'} = f, \quad \frac{\partial x_1}{\partial \delta'} = -f_1, \quad \begin{matrix} x \rightarrow y, z \\ \delta' \rightarrow \alpha' \end{matrix}$$

For spacecraft not far away from each other, the values of  $f$  and  $f_1$  should be fairly close. Thus, errors in  $\alpha'$  and  $\delta'$  will cancel implicitly. Results of the Viking demonstration that are to be discussed later show that most of the simulated Mars ephemeris error (2000 km) was removed only when both spacecraft were estimated.

The comparison in the lower chart of Fig. 2 reveals the same conclusion as in Ref. (2) that dual spacecraft data types are not sensitive to platform parameters. The degree of error cancellation depends on the angular separation between the two spacecraft.

The information content and major error sensitivities of the four kinds of data types discussed earlier may be summarized in the table in Fig. 3. It clearly shows that the dual spacecraft 4-station data type is the best as far as the data quality is concerned. However, the information content is also decreased as a result of the double differencing process when the differential range and range rate ( $\Delta\rho, \Delta\dot{\rho}$ ) information, which are highly sensitive to the planet gravitation acceleration, are removed. How to select and combine the proper data types to maximize the navigation capability depends on various conditions such as the geometry of the trajectories of the two spacecraft, Sun-Earth-probe angle and the magnitude of unmodeled spacecraft accelerations, etc.

### III. A Demonstration Conducted with Viking Spacecraft

#### A. Geometry of the Viking 2 Approach Trajectory

The two Viking spacecraft were launched in late August 1975 and arrived at Mars in the summer of 1976. When the

Viking 1 spacecraft went into orbit about Mars on June 19, 1976, Viking 2 was about 40 days away from the planet. Thus, during this last month of the approach phase of Viking 2, the technique of dual spacecraft tracking could be used to tie Viking 2 spacecraft to the planet through Orbiter 1. Figure 4 shows the approximate geometry of the two spacecraft. It reveals two of those navigation difficulties mentioned previously. First, the relatively small Sun-Earth-probe (SEP) angle increases the data noise caused by active solar plasma effects. Secondly, the long geocentric distance makes the errors in station locations significant. In addition, the low declination ( $\delta \approx 5$  deg), which cannot be seen from the figure, gives another difficulty in orbit determination. Consequently, these error sources caused the navigation uncertainty using conventional data to be as large as 1100 km, as will be discussed later. During the last two weeks of the approach phase of the second spacecraft, the angular separation between the two spacecraft was very small being 0.15 deg. Thus good cancellation of both transmission media noise and station location errors was expected. This provided a good opportunity for the dual spacecraft technique to demonstrate its potential capability in navigation.

## B. Strategy

The success of the interplanetary orbit determination effort is best measured by the accuracy of its delivered estimates for midcourse maneuvers. These estimates generally come from three independent orbit determination solutions: the long arc, the short-arc, and the optical. The optical data, although proved to be most accurate during planet approach, are not as reliable as the radiometric data. The long-arc through-maneuver solutions, according to Ref. 4, are stable, yet are not particularly accurate. The Viking 1 long-arc solutions, in fact, were in error beyond that predicted by covariance analysis. Furthermore, the long-arc solutions are computationally expensive. The short-arc solutions which contain the most up-to-date information of the spacecraft state are usually corrupted by such error sources as platform parameter uncertainties and transmission media effects, etc. The goal of this demonstration was to improve the orbit determination accuracy of the short-arc solutions with dual spacecraft data, which are relatively free of those error sources.

The data span selected for this study covers a short-arc of 8 days immediately after the last midcourse maneuver of Viking 2. The data arc stops 3 days before the MOI of Viking 2 occurred on August 7, 1976. During this period, Viking 1 was in orbit around Mars for many revolutions and its orbits were well determined relative to the planet. Thus the dual spacecraft tracking data from this eight-day arc may

accurately tie the second spacecraft to Mars and consequently improve the estimate for the final MOI delivery one day before the event. The improvement in orbit determination accuracy of this short-arc may be of great benefit to navigation if it is done in real time.

A carefully designed demonstration plan had been made and presented to the Viking Flight Path Analysis Group for support before the two spacecraft were launched in 1975. The request for dual spacecraft tracking data including 2-station and 4-station data types was not successful due to the strong resistance to any non-mission activities. As a result, the data base used for this demonstration is whatever the Viking mission requested and was available during this period. The data distribution for the dual spacecraft 2-station data is relatively poor, particularly for dual spacecraft 2-station range, compared to that of convention data (Fig. 5). Unfortunately the dual spacecraft 4-station Doppler was not scheduled during the entire Viking mission.

## C. Algorithm of Data Processing

An algorithm for processing dual spacecraft data was briefly explained in Ref. 2. This algorithm generates new data types by differencing conventional data files (ACCUME FILES) obtained from orbit determination runs made for each spacecraft separately. The new file contains the differenced data types and the conventional data from the second spacecraft. The partial derivatives for the state and other parameters of the referenced spacecraft are included. For dual spacecraft 2-station range and doppler, they may be expressed by the following form of differential correction.

$$\Delta \rho_{2\ S/C} = \Delta \rho - \Delta \rho_o = \frac{\partial \rho}{\partial q_i} \Delta q_i - \frac{\partial \rho_o}{\partial q_{oi}} \Delta q_{oi} \quad (9)$$

$$\Delta \dot{\rho}_{2\ S/C} = \Delta \dot{\rho} - \Delta \dot{\rho}_o = \frac{\partial \dot{\rho}}{\partial q_i} \Delta q_i - \frac{\partial \dot{\rho}_o}{\partial q_{oi}} \Delta q_{oi}$$

where

$\Delta \rho_{2\ S/C}, \Delta \dot{\rho}_{2\ S/C}$  are two spacecraft range and doppler residuals,

$\Delta \rho, \Delta \dot{\rho}$  are range and doppler residuals of the trailing spacecraft,

$\Delta \rho_o, \Delta \dot{\rho}_o$  are range and doppler residuals of the leading or reference spacecraft.

$q_i$  and  $q_{oi}$  are parameters that affect the trajectory of the trailing and reference spacecraft respectively, and they may be expressed as:

$$q_i = \begin{bmatrix} X \\ Y \\ P \end{bmatrix} \quad q_{oi} = \begin{bmatrix} X_o \\ Y_o \\ P_o \end{bmatrix}$$

where

$X$  = state of the trailing spacecraft

$X_o$  = state of the leading (reference) spacecraft

$Y$  = dynamical parameters (such as unmodeled spacecraft accelerations, etc.) of the trailing spacecraft

$Y_o$  = dynamical parameters of the leading spacecraft

$P$  = nondynamical parameters (such as station locations, etc.) of the trailing spacecraft

$P_o$  = nondynamical parameter of the leading spacecraft.

The procedure for data processing and differencing may be seen from Fig. 6. The computer program "DIFFER" differences the two data files (ACCUME) and creates new data types as defined by Eq. (9). The names of state and other dynamical parameters of the reference spacecraft ( $X_o$ ,  $Y_o$ ) in the new data file (REGRES) are changed to 'X1', 'Y1'... 'ATARI'... etc. that are different from the corresponding parameters of the second spacecraft. Calibrations for transmission media effects and other types of adjustments are applied to the "computed" observables during the differencing. Thus they should not be applied to the new data file later during differential corrections using dual spacecraft data.

In the previous analysis (Ref. 2), the six state parameters of the reference spacecraft were not estimated, but their errors were considered. Results of the analytical expansions suggest that both spacecraft should be estimated in the presence of large ephemeris error. In this study the referenced spacecraft was first considered and then estimated.

When the state of the referenced spacecraft  $X_o$  is considered, the covariance (considered) from the solution of the best estimate using flyby or long arc conventional data should be used as the *a priori* covariance for  $X_o$ . The cancellation of station location errors in dual spacecraft tracking depends on the knowledge of the relative locations at each complex.

According to the results of geodetic survey and short baseline VLBI<sup>1</sup> determinations, the current station location coordinates used in the orbit determination program are accurate to better than 15 cm in relative locations within a site. This information may be incorporated into the *a priori* covariance for the desired cancellation of station location errors. The correlations between near-by stations used in this analysis may be shown by the following matrix:

$$\text{A priori values} = \begin{bmatrix} r_{s_{11}} & r_{s_{14}} & \lambda_{11} & \lambda_{14} & r_{z_{11}} & r_{z_{14}} \\ 2.25D-6 & 2.44875D-6 & 0 & 0 & 0 & 0 \\ 0.99944 & 2.25D-6 & 0 & 0 & 0 & 0 \\ 0 & 0 & 9.D-10 & 8.995D-10 & 0 & 0 \\ 0 & 0 & 0.99944 & 9.D-10 & 0 & 0 \\ 0 & 0 & 0 & 0 & 2.25D-4 & 2.24995D-4 \\ 0 & 0 & 0 & 0 & 0.999978 & 2.25D-4 \end{bmatrix}$$

Correlations are shown in the lower left triangle, and

$r_{s_{11}}, r_{s_{14}}$  = distance off spin axis of DSS 11 and DSS 14 in km

$\lambda_{11}, \lambda_{14}$  = longitude of DSS 11 and DSS 14 in degrees

## IV. Results and Discussion

The orbit period of the Viking 1 spacecraft is about one day and 37 minutes. The current gravity model for Mars has difficulty in fitting the Doppler data longer than one revolution. Even for a two revolution continuous fit, the linearized residuals are considerably larger than that of the single revolution fit. The large residuals due to gravity anomalies will eventually corrupt the estimate of the second spacecraft through the two spacecraft data. This effect may be minimized by data processing strategies or stochastic models, etc. Two different attempts were tried in processing these 8-day dual spacecraft data.

### A. Reference Spacecraft is Considered

In the first attempt, the reference trajectory which consists of 8 revolutions of the orbiter was obtained from the Viking Flight Path Analysis Group (Ref. 5). Each revolution was fitted individually with 1-1/2 hours of data before and after the periapsis passage deleted. These 8 orbits of data were combined by allowing small discontinuities ( $\Delta r \approx 1$  km,  $\Delta \dot{r} \approx 1$  m/sec) between revolutions. This pseudo continuous best fit orbit was used as the reference orbit. Then the two-spacecraft data were generated by differencing the data from the orbiter and the data from the second spacecraft. The B-plane predictions based on the two-spacecraft data and the conventional

<sup>1</sup>Very long baseline interferometry

data of the same data arc were plotted in Fig. 7. Compared with the current best estimate (CBE), the predictions using two-spacecraft data had no improvement over the conventional data. According to the charged particle calibration studies (Ref. 6), most of the 1100 km error was caused by the relatively high solar plasma noise present in the 8 days of conventional data. It seems to imply that the plasma effect was not removed by differencing. A careful investigation of the Doppler residuals of both trajectories helped to discover that significant noise due to solar plasma exists in the data of the second spacecraft, but does not exist in the after-fit residuals of the orbiter. This is true particularly on August 2 when the solar noise caused a range change of about 10 m in less than 6 hours (Fig. 8). The resulting effect in doppler is as large as 16 mHz with a 8.5-mHz bias in that pass of data from the second spacecraft. While in the same pass of data of the reference spacecraft the bias is -2.2 mHz. It strongly suggests that the single revolution fit of the orbiter data absorbed the plasma noise, thus there is little or no cancellation during the differencing. When this particular pass of data was deleted, the B-plane prediction using two spacecraft data moved closer to the CBE by 600 km. This seems to confirm the above speculation. Therefore, we may conclude that for this particular case this is not the proper procedure to process 2-spacecraft data. The large plasma effects, which occurred during the last few days of the approach phase, have made this demonstration very rewarding.

The experience gained in the first attempt suggests that differencing of the two data types should take place before the orbit-by-orbit differential corrections of the reference spacecraft. In other words, the two spacecraft should be estimated simultaneously using differenced dual spacecraft data to prevent the absorption of plasma signature by the single orbit fit.

## B. Both Spacecraft are Estimated

In the second attempt, the 12 state parameters of the two spacecraft were estimated by treating the state of the reference spacecraft, the orbiter, as nondynamic stochastic parameters. The batch size is equal to the orbit period with zero correlation time. This procedure removes unmodeled gravity errors in the same manner as the single revolution fit. The orbiter data were first processed with a continuous 8-day or 8-revolution nominal trajectory with reasonably good initial conditions. Then the two-spacecraft data were differenced, and the common plasma noise was expected to cancel. The residuals of the differenced data were still considerably large (10th to 100th of a hertz) due to the inadequacy of the gravity model for a longer time span. This would be refined by the sequential estimation of the state of the first spacecraft as mentioned earlier. It was found that this method of data processing had not only successfully removed the plasma noise but had also

effectively taken care of the unmodeled accelerations caused by the Mars gravity field.

As mentioned earlier, the Viking 2 target plane (B-plane) prediction based on 8 days conventional doppler and range was badly corrupted by solar plasma effects and the error was as large as 1100 km. After the second attempt of processing the two-spacecraft data, as described in the above paragraph, the plasma noise was largely removed and the new data type which covers the same 8-day arc gave a B-plane prediction only 170 km away from the post MOI best estimate (Fig. 9). This nearly seven-times improvement in accuracy using actual two spacecraft tracking data is consistent with the results from earlier simulation analysis (Ref. 2), and it clearly reveals the potential capability of this new data type.

A series of B-plane predictions based on various combinations of data weights and data types were tried. The three predictions based on two spacecraft data shown by triangles in Fig. 9 represent three different data combinations. The one that has best agreement with the CBE is from the solution weighting the two spacecraft doppler at 0.015 Hz (1 mm/s) and two-spacecraft range at 20 m. When loosely weighted conventional data (doppler at 0.15 Hz and range at 1 km) are included, the change in the B-plane prediction is small. However, as the data weight of the conventional doppler is increased, the solution moves away from the CBE and agrees better with the solution using conventional data alone. This is because the plasma noise which is present in conventional data will start to show its effect when such data are relied on more heavily. When the two spacecraft range is dewighted by a factor of 10 (to 200 m), the prediction using two spacecraft doppler and range moved slightly away from the CBE. The agreement is still better than 300 km. The linearized residuals of the differenced two spacecraft doppler with 10-min count time are reasonably small with pass-by-pass noise of about 0.003 to 0.004 Hz.

It is also important to examine the time history of B-plane improvements of using the new data type. Figure 10 shows the comparison of B-plane prediction between long and short arc solutions of conventional data and the short arc solutions of dual spacecraft data. This comparison clearly demonstrates the following facts:

- (1) The short-arc dual spacecraft solutions are linearly converging to the current CBE. This shows the stability of the new data type.
- (2) At one day before the final MOI delivery, dual spacecraft data give more accurate prediction than conventional data.
- (3) Dual spacecraft tracking has the potential of significantly reducing DSN tracking time requirements.

Therefore, one may conclude that with limited data the two spacecraft tracking technique is able to improve the navigation accuracy by nearly a factor of 7 in the presence of significant space plasma noise and under the unfavorable geometry of low declination. The insensitivity to ephemeris errors cannot be demonstrated by comparing with the standard Viking solutions because of the accurate knowledge of Mars ephemeris ( $\leq 30$  km). To enhance our understanding of this capability, a large error was introduced to the Mars ephemeris and the results will be discussed next.

### C. Improvements Under Simulated Mars Ephemeris Error

An actual error of about 2000 km in Mars position (1000 km in range, 1000 km downtrack and 1500 km out of plane), which is about the current uncertainty of the planet Saturn, was introduced in the ephemeris (DE84) by Newhall (Ref. 5). Then the data from the Viking approach phase (same 8 day arc) were processed in the same way as the second attempt; i.e. both spacecraft were estimated. Large residuals were induced both in doppler data (100th to 10th of a hertz) and in range data (70 km in Viking B spacecraft and 1000 km in Viking A spacecraft) as a result of the 2000 km ephemeris error. The resulting B-plane error after fitting the 8 days of conventional data (state only) is as large as 11,000 km using doppler only and 20,000 km with range included. When Mars ephemeris parameters are estimated, the errors become even larger. This is believed to be due to the fact that this 8-day arc which ends 3 days away from Mars encounter does not have enough information to estimate the 12 extra ephemeris parameters. The differenced two-spacecraft data together with loosely weighted conventional doppler helped to bring the B-plane prediction to within 400 km of the CBE as seen in Fig. 11. Two other solutions using two spacecraft data are all less than 800 km away from the best estimate. The linearized residuals of the two spacecraft data are as small as that of the previous case without the large ephemeris error. This more than 10 times improvement both in B-plane predictions as well as in

data noise clearly shows the insensitivity of the two-spacecraft data to large ephemeris error. This particular advantage of two-spacecraft navigation will be very useful for future missions to the outer planets with large ephemeris errors such as Saturn, Uranus, etc.

## V. Conclusions

The potential improvements in navigation capability of dual spacecraft tracking have been successfully demonstrated using Viking approach data. Under unfavorable conditions of low SEP, low declination and large Earth-spacecraft distance, the dual spacecraft tracking technique improved the Viking 2 approach accuracy, by a factor of 7, to less than 200 km at MOI-2 days. Results also reveal the potential reduction of tracking time requirements during planet approach. The 8-day solution of dual spacecraft tracking yields slightly better B-plane prediction than the 40-day solution of conventional data. From the results of the analytical expansion and the Viking demonstration with a large intentional Mars ephemeris error, we are able to conclude that dual spacecraft data types are insensitive to ephemeris error.

## VI. Recommendations for Further Study

As a result of this analysis, the following recommendations are proposed:

- (1) Examine the potential benefits of dual spacecraft tracking for future missions involving two spacecraft.
- (2) Conduct demonstrations of dual spacecraft tracking when the leading spacecraft is a flyby rather than an orbiter.
- (3) The dual spacecraft 4-station doppler data type should be included in the demonstration.
- (4) Modify and standardize the prototype software for operational use.

## Acknowledgements

The author would like to give sincere thanks to J. Campbell, E. Christensen, J. Ellis, C. Hildebrand, X. Newhall, J. Ondrasik, G. Rinker, and H. Siegel for their help in the processing and analyzing of the Viking data.

Thanks are also due to R. Rudd and R. Hastrup for their effort in extending tracking coverage for dual spacecraft study, and to S. Finley for programming support.

Special thanks to J. McDanell for many helpful discussions and suggestions.



## References

1. Preston, R. A., "Dual Spacecraft Radio Metric Tracking," *DSN Progress Report*, 42-22, May/June, pp. 51-65.
2. Chao, C. C., V. J. Ondrasik, and H. L. Siegel, "Improvements in Navigation Resulting from the Use of Dual Spacecraft Radiometric Data," AIAA Paper 76-834 presented at the AIAA/AAS Astrodynamics conference held at San Diego, California, August 18-20, 1976.
3. Hamilton, T. W., and W. G. Melbourne, "Information Content of a Single Pass of Doppler Data from a Distant Spacecraft," in *The Deep Space Network*, Space Programs Summary 37-39, Vol. 3, pp. 18-23, JPL, May 31, 1966.
4. Rourke, K. H., et al., "The Determination of the Interplanetary Orbits of Viking 1 and 2," AIAA Paper 77-71 presented at the AIAA 15th Aerospace Science meeting held at Los Angeles, California, January 24-26, 1977.
5. Hildebrand, C. E., et al., "Viking Satellite Orbit Determination," AIAA Paper 77-70, presented at the AIAA 15th Aerospace Science meeting held at Los Angeles, California, January 24-26, 1977.
6. Yip, K. W., F. B. Wim, and S. C. Wu, "Viking 1 S/X Dual Doppler Demonstration," EM 391-53, July 28, 1976 (JPL internal document).
7. Newhall, X. X., private communication.

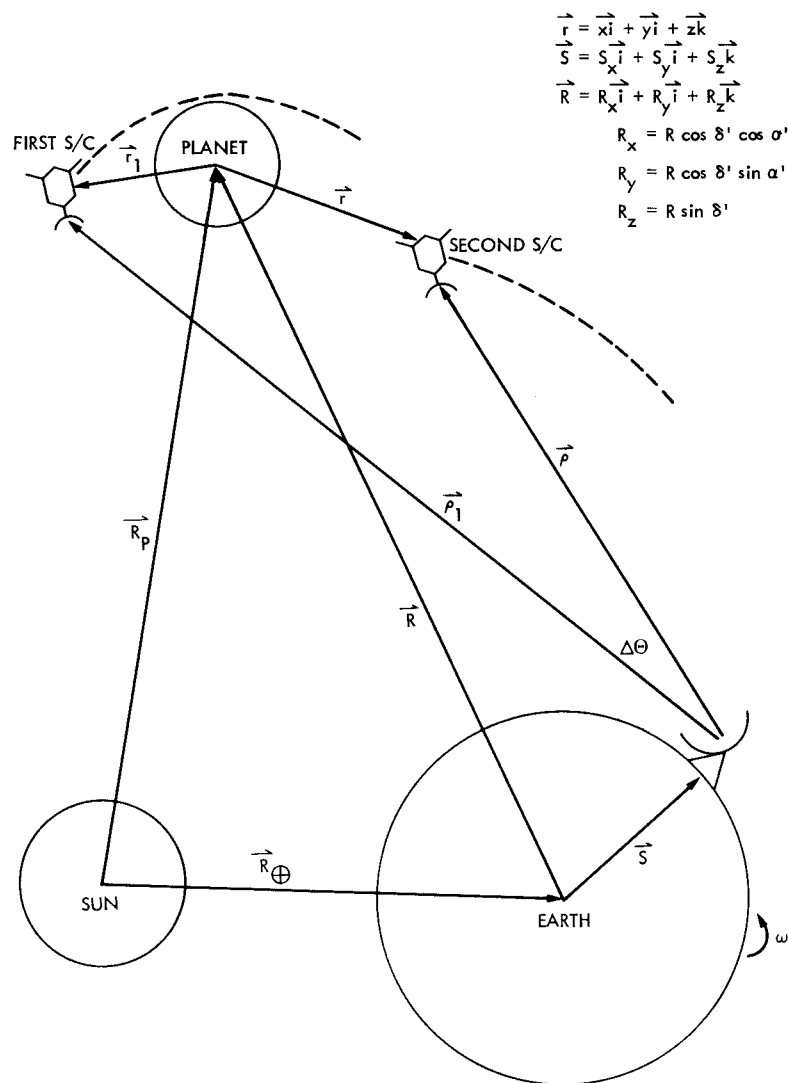
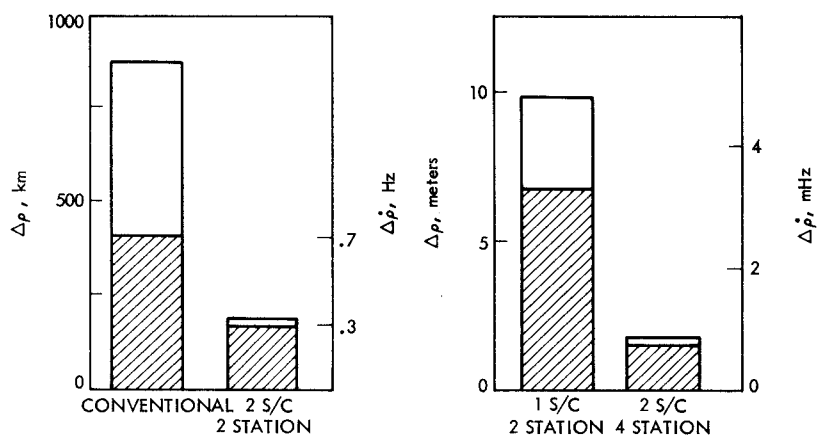
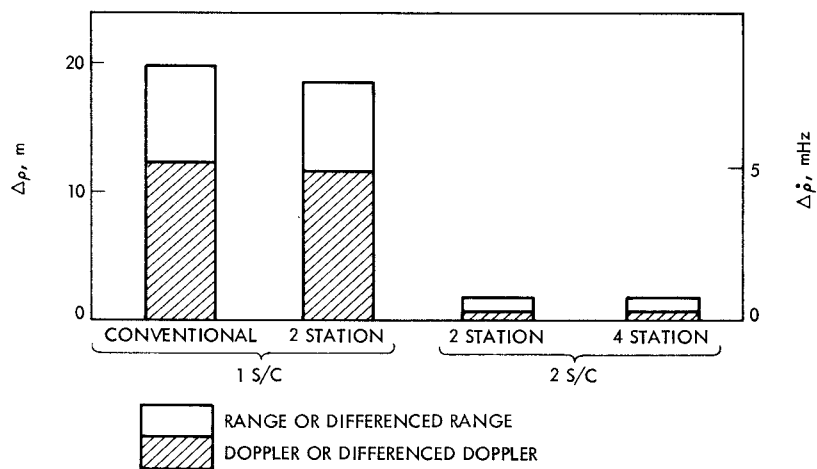


Fig. 1. Geometry of dual spacecraft fly-by of a planet

(a) ASSUMED SATURN EPHEMERIS ERRORS:  $\Delta r = 800$  km,  $\Delta \alpha = \Delta \delta = 1500$  km  
at  $\delta = 0^\circ$  and  $\Delta \theta = 9^\circ$



(b) ASSUMED STATION LOCATION ERRORS:  $\Delta r_s = 3$  m,  $\Delta \lambda = 5$  m,  $\Delta z = 15$  m,  
and ( $\Delta \theta = 9^\circ$ )



**Fig. 2. Bias induced in observables due to assumed errors in ephemeris and station location**

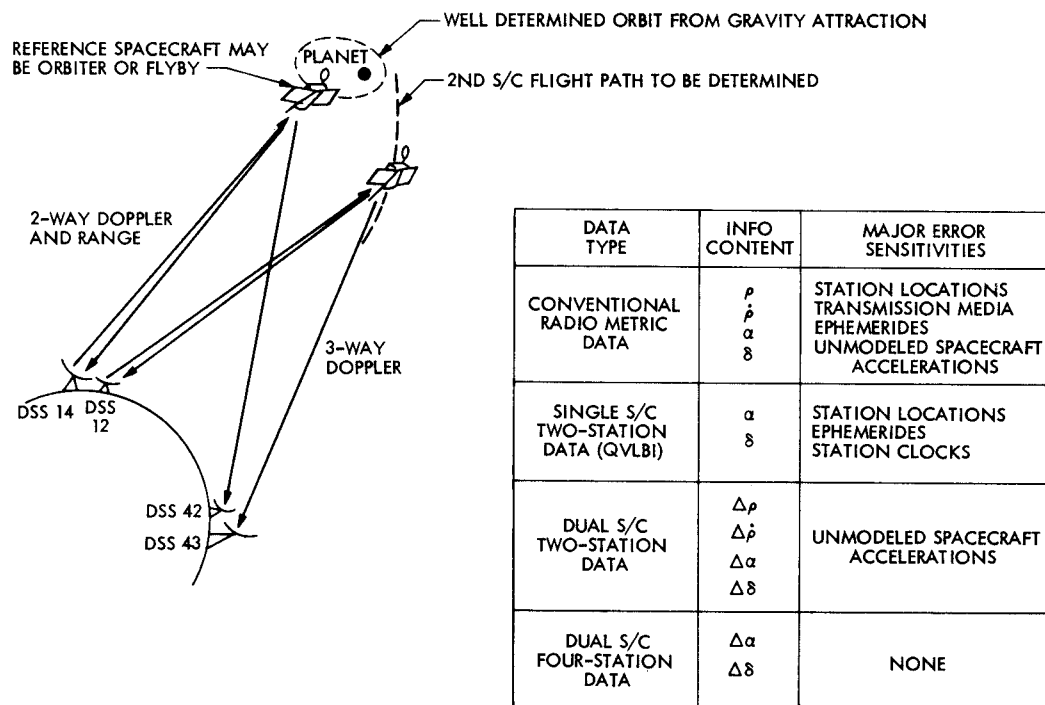


Fig. 3. Dual spacecraft tracking concept and data types

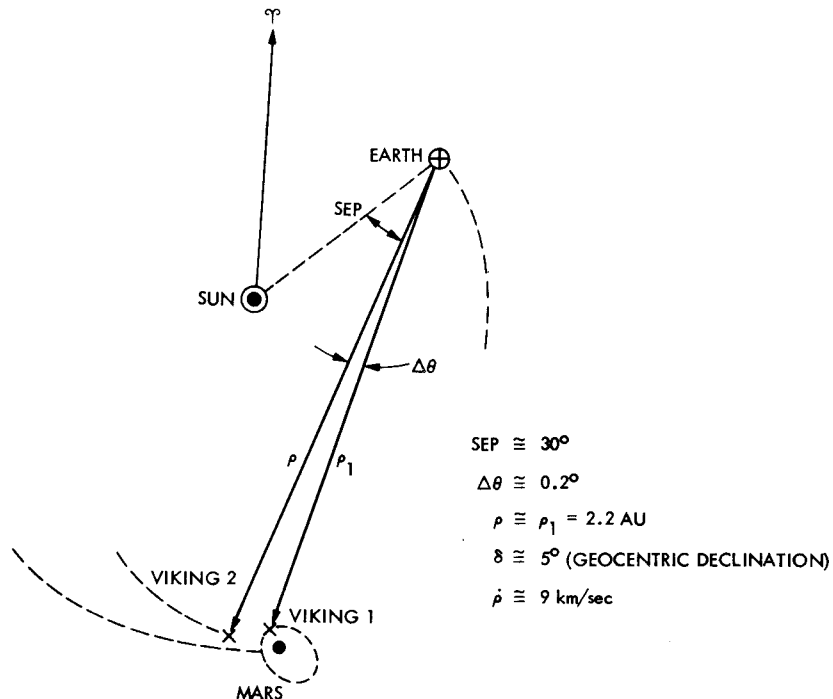


Fig. 4. Projection of approximate heliocentric trajectories in ecliptic plane during the approach of Viking B spacecraft

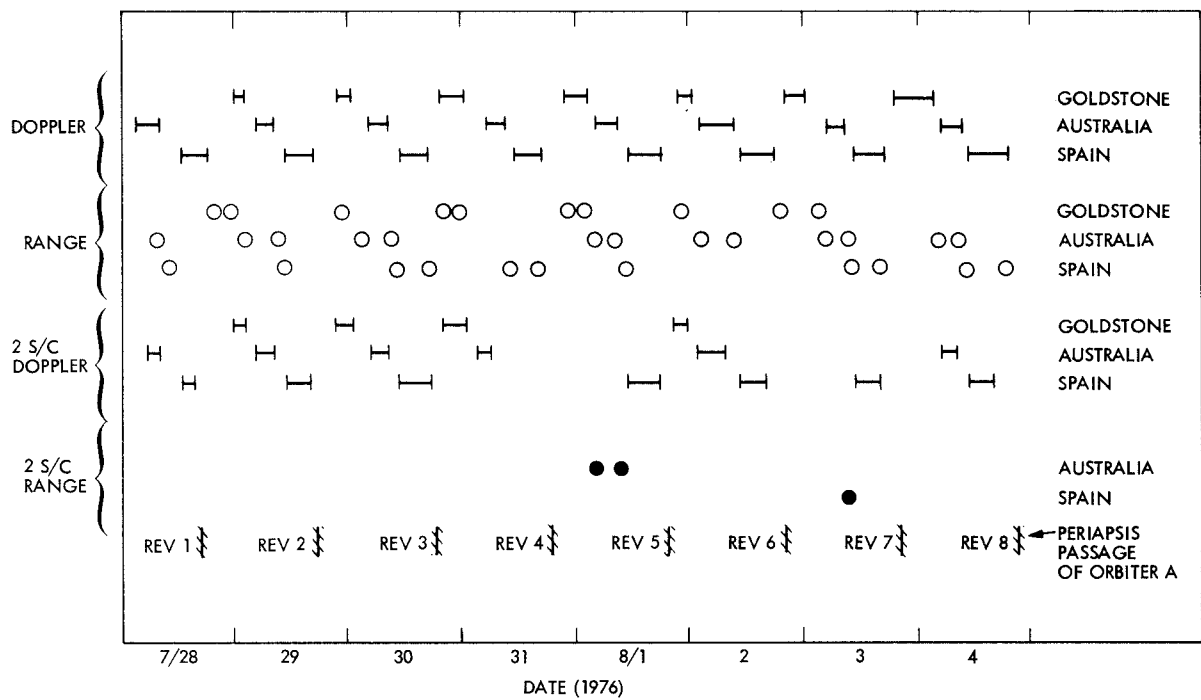
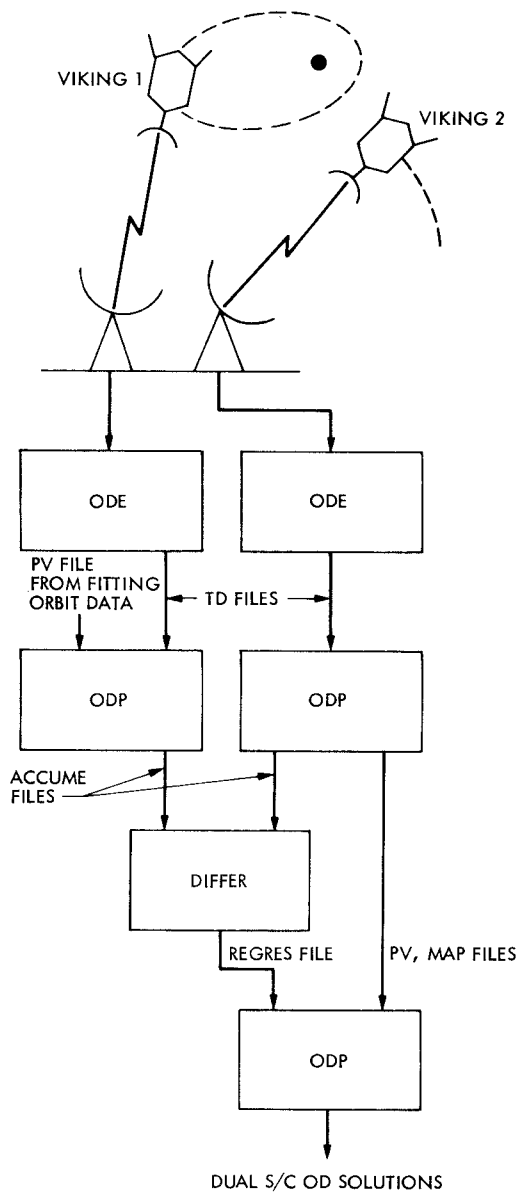


Fig. 5. Data distribution of dual spacecraft and conventional data types



A MODIFIED VERSION OF ODE MAINTAINS  
DOPPLER SIMULTANEITY AFTER DATA  
EDITING AND COMPRESSION

STANDARD ODP COMPUTES OBSERVABLES  
PV FILE, PARTIAL DERIVATIVES AND  
ATMOSPHERE CALIBRATIONS

DIFFERENCE 2 S/C DATA AND USE 'X1', 'Y1' . . .  
AND 'ATARI' . . . FOR PARAMETERS OF THE  
REFERENCE S/C

ATMOSPHERE CALIBRATIONS SHOULD  
NOT BE APPLIED HERE

**Fig. 6. Dual spacecraft orbit determination software interfaces**

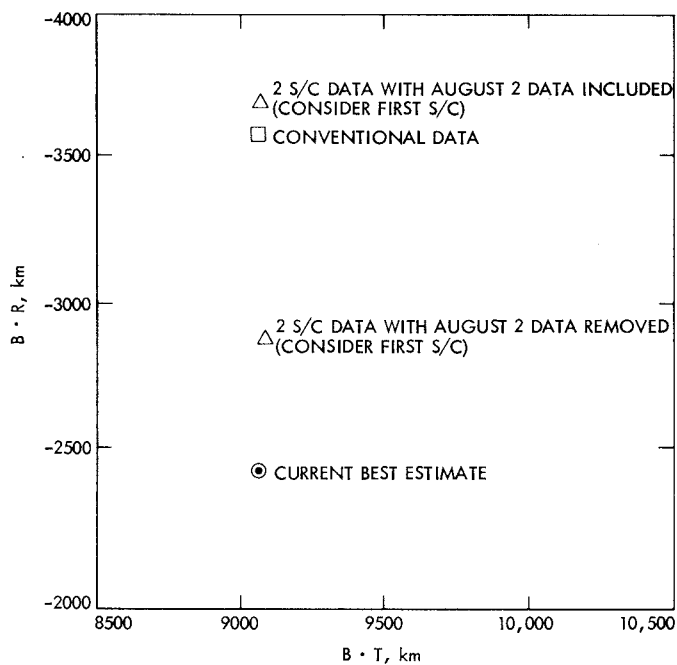


Fig. 7. Viking 2 B-plane predictions at MOI-3 day with 8 days of data

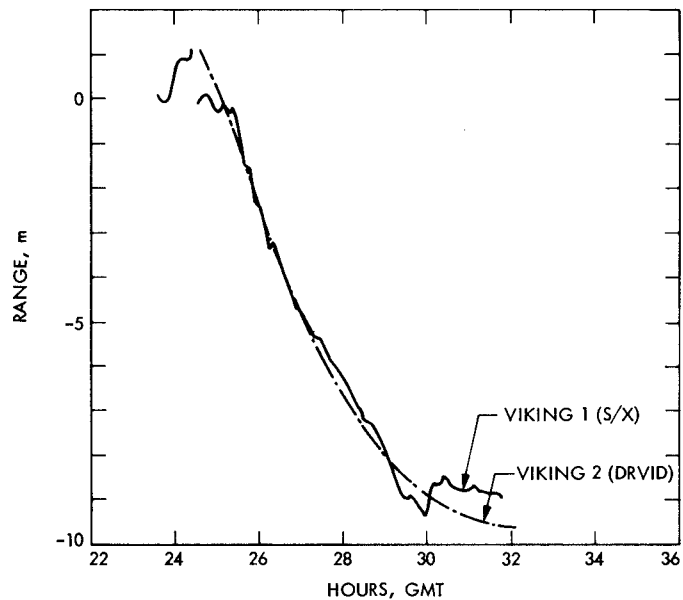


Fig. 8. One-way range change due to charged particle effect on August 2, 1976

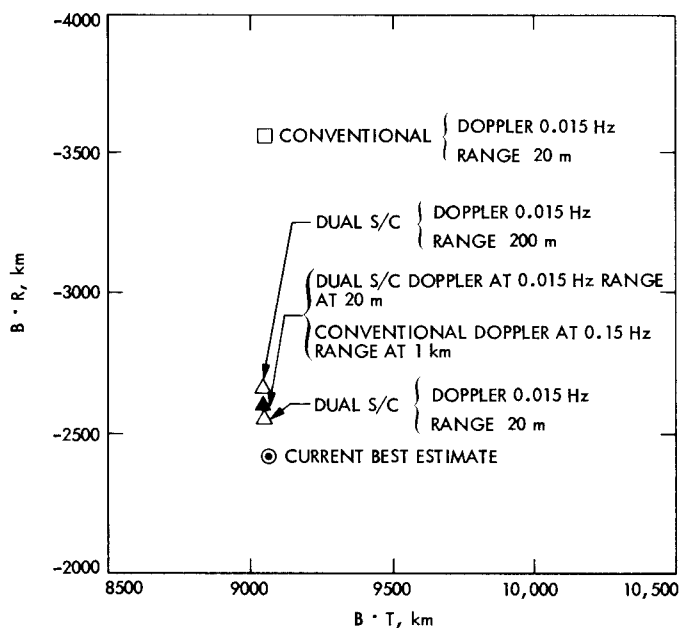
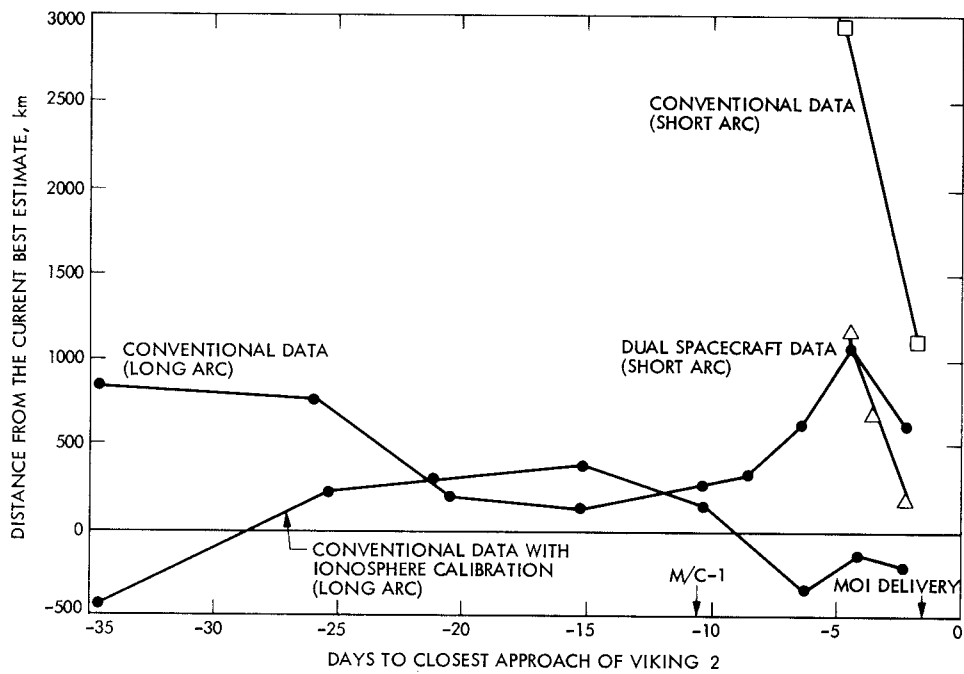


Fig. 9. Viking 2 B-plane predictions at MOI-3 day with 8 days of data



**Fig. 10. History of navigation improvement from dual spacecraft tracking**



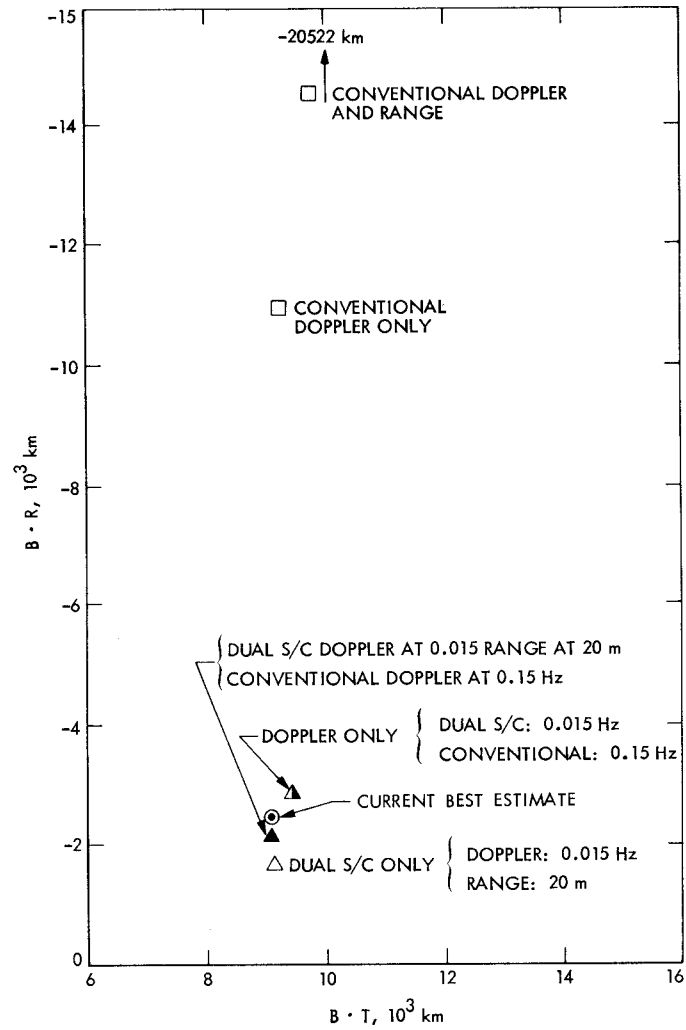


Fig. 11. Viking 2 B-plane predictions at MOI-3 day with 8 days of data in the presence of large ephemeris error (2000 km)